Food and Bioprocess Technology (2020) 13:1421–1434
https://doi.org/10.1007/s11947-020-02483-0

ORIGINAL RESEARCH

Studies on the Binding Interactions of Grass Carp (*Ctenopharyngodon idella*) Myosin with Chlorogenic Acid and Rosmarinic Acid

Yuan Huang[1] · Hongying Du[1,2] · Ghulam Mustafa Kamal[3] · Qiongju Cao[1] · Chen Liu[1] · Shanbai Xiong[1,2] · Anne Manyande[4] · Qilin Huang[1,2]

Received: 2 April 2020 / Accepted: 17 June 2020 / Published online: 27 June 2020

Abstract

There are many polyphenols used for the preservation of fish, but the interaction mechanism between polyphenols and fish protein is rarely reported. In the present study, the interactions between two kinds of polyphenols (chlorogenic acid (CGA) and rosmarinic acid (RA)) and the myosin of grass carp (*Ctenopharyngodon idella*) were explored using multi-spectroscopic techniques. Both CGA and RA were found to be involved in reducing the intrinsic fluorescence and surface hydrophobicity of myosin and increasing the UV absorption intensity. This indicates that interactions between CGA, RA, and myosin ultimately result in the formation of polyphenol-myosin complexes. The binding process of CGA and RA for the formation of the complex was spontaneous. The main binding forces between RA and myosin are hydrogen bonding and van der Waals forces, whereas hydrophobic interactions were observed between CGA and myosin. The results of circular dichroism (CD) showed that the presence of CGA and RA increased the content of myosin alpha-helix. CGA and RA caused myosin aggregation which reduced the corresponding solution dispersibility. CGA and RA protected the myosin sulfhydryl groups and reduced the degree of their oxidation. Furthermore, the complexes formed by the combination of myosin, CGA, and RA exhibited the strongest synergistic antioxidant properties than any one of them. The findings of the present study provide insights into our understanding of the mechanism of interactions between myosin and polyphenols which could provide information on the application of polyphenols in preserving aquatic products.

Keywords Grass carp · Myosin · Chlorogenic acid · Rosmarinic acid · Spectroscopic techniques · Fluorescence

Introduction

As a common freshwater fish, grass carp (*Ctenopharyngodon idellus*) is very popular with consumers for its pleasant taste, rich nutritional value, and low price. With the development of the cold chain and fresh supermarket industry as well as improvement in lifestyle of the new generation, fresh fish fillets have gradually replaced live fish as the major marketing strategy (Yu et al. 2017). However, due to frequent lipid oxidation and protein degradation during storage, fresh grass carp fillets are prone to deterioration and thus have a shorter shelf life compared with live fish (Wu et al. 2018). Therefore, it is vital to find ways of improving the shelf life of grass carp fillets.

Bio-based coatings and films combined with refrigeration have been widely considered effective and environmentally friendly methods of improving the fish fillets' shelf life (Reesha et al. 2015). In general, the materials used in the bio-based coatings and films are mainly carbohydrates, protein gels, and natural plant extracts (Yu et al. 2018). For instance, pullulan has been used to inhibit myofibrillar protein degeneration and maintain Ca^{2+}-adenine pyrophosphatase (Ca^{2+}-ATPase) activity in chilled grass carp (Jiang and Wu

✉ Hongying Du
hydu@mail.hzau.edu.cn

✉ Qilin Huang
hql@mail.hzau.edu.cn

[1] College of Food Science and Technology, Huazhong Agricultural University, Wuhan 430070, Hubei, People's Republic of China

[2] National R & D Branch Center for Conventional Freshwater Fish Processing, Wuhan 430070, Hubei, People's Republic of China

[3] Department of Chemistry, Khwaja Fareed University of Engineering and Information Technology, Rahim Yar Khan 64200, Pakistan

[4] School of Human and Social Sciences, University of West London, Middlesex TW8 9GA, UK

2018). Chitosan has also been wildly used as a preservative in maintaining the quality and extending the corresponding shelf life of many varieties of fish fillets such as silver pomfret (*Pampus argentus*) (Wu et al. 2016), sea bass (*Lateolabrax japonicus*) (Qiu et al. 2014), grass carp (*Ctenopharyngodon idella*) (Yu et al. 2017), and rainbow trout (*Oncorhynchus mykiss*) (Ojagh et al. 2014). Fish gelatin coating can effectively reduce total volatile basic nitrogen, peroxide value, thiobarbituric acid value, and pH of refrigerated rainbow trout and thus extend its shelf life (Hosseini et al. 2016).

Recently, some natural plant extracts with excellent antioxidant and antibacterial properties such as polyphenols have been used in preserving fish products (Luan et al. 2017). Tea polyphenols are currently the most widely studied polyphenol which can inhibit the oxidation and degradation of proteins during preservation (Feng et al. 2017). Apple polyphenol was applied in synthesizing fresh-keeping films for preserving fish (Sun et al. 2018). It is reported that brown seaweed polyphenols and α-tocopherol contribute to the reduction of the degree of protein oxidation and maintenance of the texture characteristics of frozen fish meat compared with the traditional antioxidant, ascorbic acid (Wang et al. 2017). Due to their excellent preservation effects, the application of polyphenols in the preservation of fish products has also become one of the research hotspots (Rodríguez et al. 2012; Cao et al. 2019).

It has been reported that myosin degradation is a key factor involved in accelerating the deterioration of aquatic products (Daskalova 2019). Numerous studies on the application of polyphenols to fish preservation are available in literature, and most of them focus on assessing their preservation performance. However, there are very few studies available that have reported the interaction between myosin and polyphenols for the purpose of demonstrating the preservation of products. In other words, polyphenols have been used in the inhibition of fish protein degradation, but the mechanism is not yet clear (Fan et al. 2008). Therefore, the present study intends to explore the mechanisms involved in the interaction between myosin of grass carp muscle, chlorogenic acid (CGA), and rosmarinic acid (RA), respectively by employing multi-spectroscopic techniques. It is well-known that spectroscopic techniques are convenient and meticulous when studying the interactions between small molecules and proteins to better understand the interaction process between them. For example, the data of fluorescence spectroscopy shows that quenching processes of CGA with whey protein and casein are static (Jiang et al. 2018); 8-anilino-l-naphthalene sulfonic acid (ANS) as a hydrophobic fluorescent probe is utilized to study the effect of flavonoids on the surface hydrophobicity of β-lactoglobulin (Li et al. 2018).

Results obtained by this study will offer some new insights to our understanding of the mechanism of polyphenols in preserving aquatic products based on the binding modes between polyphenols and myosin.

Materials and Methods

Materials

Bovine serum albumin (BSA) was obtained from Sigma-Aldrich Chemical Co. (St. Louis, MO, USA). 8-Anilino-1-naphthalenesulphonic acid (ANS) was acquired from Aladdin Reagents Co., Ltd. (Shanghai, China). Chlorogenic acid (CGA, purity > 98%) and rosmarinic acid (RA, purity > 98%) standards were provided by Shanghai Yuanye Biological Technology Co., Ltd. (Shanghai, China). All other chemicals used were of analytical grade and purchased from SinoPharm Chemical Reagent Co., Ltd. (Shanghai, China). All aqueous solutions were prepared using deionized water.

Methods

Myosin Preparation

Live grass carps (*Ctenopharyngodon idella*) with an average weight of 5–6 kg were purchased from Huazhong Agricultural University market (Wuhan, China) and transported alive in a plastic bag to the laboratory within 20 min. The live fish (n = 10) were immediately sacrificed by a blunt instrument to the head, viscera removed and washed with tap water. The fresh white muscle was separated manually from the back muscle and kept at 4 °C for no longer than 1 h (for sample preparation and instrument setting) for further myosin preparation. Myosin was extracted from the white muscle of the fresh grass carp according to the method used by Park and Lanier with some modifications (Park and Lanier 1989). Briefly, firstly, in order to remove residual blood and water-soluble proteins, and obtain myofibrillar protein, the muscle was minced through a food processor (Braun K600, Braun GmbH, Germany) and mixed with ten-fold volume of solution A (0.10 M KCl, 0.02% sodium azide, and 20 mM Tris-HCl buffer, pH 7.5). Then the mixture was homogenized using an inline dispersing homogenizer (Model FJ-200, Shanghai specimen and models factory, China) operated at a speed setting of 9000 rpm for 1 min. The homogeneous liquid was incubated for 15 min at 4 °C and centrifuged at 8000 rpm for 5 min in a high-speed refrigerated centrifuge machine (Beckman Avanti J-20XP, America). Secondly, to separate myosin and actin, the sediment was suspended with 5 times volume solution B (0.45 M KCl, 5 mM β-mercaptoethanol, 0.2 M $Mg(COO)_2$, 1 mM EGTA, and 20 mM Tris-HCl buffer, pH 6.8), mixed with adenosine 5′-triphosphate (ATP) to a final concentration of 5 mM and incubated for 1 h at 4 °C. Then, the mixture was centrifuged at 12,000 rpm for 10 min. Finally, purification of crude myosin was performed. The final supernatant was diluted slowly with 10 times the volume of 1 mM $KHCO_3$ and kept at 4 °C for 15 min, and the mixture was centrifuged at 12,000 rpm for 10 min at 4 °C. After that,

the precipitate was re-suspended with 2.5 times volume solution C (0.5 M KCl, 5 mM β-mercaptoethanol, and 20 mM Tris-HCl buffer, pH 7.5). The re-suspended precipitate was incubated at 4 °C for 10 min, diluted with 2.5 times volume of 1 mM $KHCO_3$, while adding $MgCl_2$ to a final concentration of 10 mM. The mixture was kept at 4 °C overnight and then centrifuged at 10,000 rpm for 15 min. The pellets were re-suspended in 0.6 M NaCl (pH 7.5) (dissolved in ionized water) and then centrifuged at 5000 rpm for 10 min. The supernatant was stored at 4 °C for use within 3 days. The protein concentration of the supernatant was determined by the Lowry method (Lowry et al. 1951), using bovine serum albumin (BSA) as a standard. The myosin concentration was adjusted with buffer D (pH = 7.5, 0.6 M NaCl and 0.02 M Tris-HCl).

Polyphenol Stock Solution Preparation

CGA and RA were dissolved in deionized water and fixed to 1 mg/mL in a brown volumetric flask to obtain the stock solutions, respectively. The polyphenol stock solutions were kept in the refrigerator at 4 °C for further use.

Fluorescence Spectroscopic Analysis

Fluorescence spectral data were recorded at three different temperatures (25 °C, 30 °C, 37 °C) by fluorescence spectrophotometer (F-4600, Hitachi, Japan) equipped with a quartz cuvette of 1.0 cm path length. The excitation spectra were obtained at 280 nm, whereas emission spectra were recorded at a wavelength ranging from 300 to 450 nm. Synchronous fluorescence spectra were collected from 260 to 350 nm at 25 °C with the wavelength interval of $\Delta\lambda = 15$ nm and $\Delta\lambda = 60$ nm (Xu et al. 2019). The sample solutions of CGA-myosin and RA-myosin for fluorescence testing were prepared by mixing myosin solution (0.5 mg/mL), different concentrations of polyphenols (0, 3, 4, 5, 6, 7, 8 μg/mL) and buffer D. The final volume of the sample solution was made up to 5 mL. The solution was thoroughly mixed and left for 30 min in the experimental temperature for measurement.

Fluorescence Data Analysis

Fluorescent quenching is measured based on the Stern-Volmer equation (Lakowicz 1999):

$$F_0/F = 1 + K_{SV}[Q] = 1 + K_q\tau_0[Q] \quad (1)$$

where F_0 is the fluorescence intensity without a quencher; F is the fluorescence intensity with a quencher, τ_0 ($\sim 10^8$ s) is the average lifetime of fluorophore without a quencher; $[Q]$ is the concentration of the quencher; K_{SV} is the dynamic quenching constant; and K_q is the biomolecule quenching rate constant. K_{SV} can be deduced from the slope of linear regressions of the curve F_0/F versus $[Q]$ and K_q is deduced from K_{SV} and τ_0, while the correlation coefficient can also be derived from the linear regression equation.

For static quenching, the relationship between the concentration of the protein and the fluorescence quenching intensity was calculated by applying the double-logarithm equation given below.

$$\log[(F_0 - F)/F] = \log K_a + n\log[Q] \quad (2)$$

where K_a is the binding constant and n is the number of binding sites per protein. So K_a can be deduced from the intercept of linear regressions of the curve $\log[(F_0 - F)/F]$ versus $(\log K_a + n\log[Q])$ and n is deduced from the slope of the linear regression, while the correlation coefficient can also be derived from the linear regression.

The entropy change (ΔS), enthalpy change (ΔH), and free energy change (ΔG) were estimated using the Van't Hoff equation (Dai et al. 2018).

$$\ln K_a = -\Delta H/RT + \Delta S/T \quad (3)$$

$$\Delta G = -RT\ln K_a = \Delta H - T\Delta S \quad (4)$$

where K_a is the binding constant and same as Eq. (2) at the corresponding temperature; R is the gas constant (8.314 J mol^{-1} K^{-1}); T is the experimental temperature (298, 303, and 310 K). The ΔS and ΔH values were acquired from the intercept and slope based on $\ln K_a$ and 1/T while ΔG value was calculated using Eq. (4), while the correlation coefficient can also be derived from the linear regression.

Circular Dichroism Spectroscopy Measurement

Secondary structures of myosin and its complexes with each polyphenol were measured by a CD spectropolarimeter (J-1500, JASCO Ltd., Japan) equipped with a 1.0-mm quartz cuvette. The CD spectra were recorded from 200 to 240 nm at 25 °C with a scanning speed of 100 nm/min, 3 accumulations, and 1 nm bandwidth (Dan et al. 2019). The CD results were expressed as mean residue ellipticity (MRE) in degree cm^2 $dmol^{-1}$ based on the Yang's method (Yang et al. 1986) provided with the spectropolarimeter through the instrument's own program. The myosin and myosin-polyphenol solution ($C_{myosin} = 0.5$ mg/mL, $C_{CGA} = C_{RA} = 8$ μg/mL) was incubated for 30 min and diluted 10 times with deionized water to a total volume of 5 mL due to the strong far UV absorption of NaCl and the need for CD test.

UV Absorption Spectra Measurement

The absorption spectra of myosin solutions (1 mg/mL) with polyphenols (1 mg/mL) at various concentrations (0, 3, 6, and 8 μg/mL) were determined using a UV-721

spectrophotometer (Shanghai Precision Instrument Co., Ltd., Shanghai, China) with a wavelength range of 200 to 400 nm and a scanning speed of 100 nm/min using D buffer as a blank.

Turbidity Measurement

The samples for turbidity measurement were prepared as described in UV absorption spectral measurement, and the turbidity values of samples were recorded as the UV absorbance at 320 nm (Yongsawatdigul and Sinsuwan 2007).

Surface Hydrophobicity Measurement

Surface hydrophobicity of myosin and complexes were recorded using a fluorescence spectrophotometer (F-4600, Hitachi, Japan) with excitation and emission wavelengths at 390 and 470 nm, respectively using 8-anilino-l-naphthalene sulfonic acid (ANS) as a fluorescent probe. The excitation and emission slit widths were set at 5 nm each. The myosin solutions (1 mg/mL) were diluted to 0.05, 0.1, 0.15, and 0.2 mg/mL using buffer D with polyphenols (1 mg/mL) at various concentrations (0, 3, 6, and 8 μg/mL). Four milliliters of each complex solution was supplemented with 20 μL of 8 mM ANS in 0.1 M potassium phosphate buffer (pH 7.0) and mixed well. After keeping each sample in the dark for 10 min, the fluorescent intensity was measured. Protein hydrophobicity was calculated from the initial slope of a plot of fluorescence intensity against protein concentration using linear regression analysis. The initial slope was defined as S_0-ANS (Karaca et al. 2011).

Particle Size Measurement

The particle size of the protein was determined using the Malvern Zetasizer Nano ZS (Zetasizer Nano ZS, Malvern Instruments, Worcestershire, UK) according to the method described by Peng et al. (2017) with slight modifications. The concentration of myosin in the sample mixture was 0.1 mg/mL, and the concentration of polyphenols was 8 μg/mL. The refractive index used for the dispersed phase was 1.450. The RI corresponding to water was 1.333, the incubator temperature was 25 °C, and the scattering angle was 173° in Malvern Zetasizer Nano ZS.

Determination of Reactive Sulfhydryl Groups

The reactive sulfhydryl (SH) groups were detected spectrophotometrically according to the method described by Liu and his colleagues (Liu et al. 2011) with little modification. Briefly, the myosin (0.5 mg/mL) was mixed with different concentrations (0, 3, 4, 5, 6, 7, 8 μg/mL) of polyphenol solutions and placed at 4 °C in refrigerator for 9 h. An aliquot (100 μL) of Ellman's reagent (10 mM 5,5-dithio-bis-[2-nitrobenzoic acid]) was added to 4.7 mL protein solution and the mixture placed the refrigerator at 4 °C for 1 h. The reactive SH was measured at 412 nm with a spectrophotometer and the content of sulfhydryl calculated using the molar extinction coefficient of 13,600 M^{-1} cm^{-1}.

Reducing Power Measurement

Following the method reported by Mohammadian and his colleague (Mohammadian and Madadlou 2016), the protein solutions of myosin (0.5 mg/mL) mixed with different concentrations of polyphenols (0, 3, 4, 5, 6, 7, 8 μg/mL) were firstly placed in the refrigerator at 4 °C for 9 h. Then, a 2 mL sample was mixed with 2 mL of phosphate buffer (0.2 M, pH 6.6) and 2 mL of potassium ferricyanide (1%). The mixture was incubated at 50 °C for 20 min. After incubation, the mixture was quickly cooled, and 2 mL of 10% trichloroacetic acid was added. Subsequently, the mixture was centrifuged at 4000 rpm/min for 10 min. An aliquot of 2 mL of the supernatant was mixed with 2 mL of deionized water and 0.4 mL of $FeCl_3$ (1%). After incubation for 10 min at room temperature, the absorbance of the resulting Prussian blue solution was recorded at 700 nm.

Statistical Analysis

All measurements were recorded in triplicate if not stated otherwise, and the data were expressed as the mean ± standard deviation (SD). Statistical analyses were performed using Microsoft Excel 2013 and IMP SPSS 22. Significant differences ($p < 0.05$) in means between the samples were separated using Duncan's Multiple Range tests. All the figures were drawn using the Origin 2018 software.

Result and Discussion

Fluorescence Spectra Analysis

Effect of Polyphenols on Myosin Fluorescence

Myosin is known to have intrinsic fluorescence mainly because of the presence of tryptophan (Trp) and tyrosine (Tyr) (Kominz et al. 1954; Yan et al. 2013). When the excitation wavelength was set at 280 nm, the changes in myosin intrinsic fluorescence without or with the different concentrations of polyphenols (chlorogenic acid, rosmarinic acid) were recorded and are presented in Figs. 1 and 2 a, b, and c, respectively. It was shown that myosin has the strongest emission peak near 334 nm, and the fluorescence intensity markedly decreased with increasing the concentration of CGA or RA. Meanwhile, the fluorescence intensity of myosin was reduced

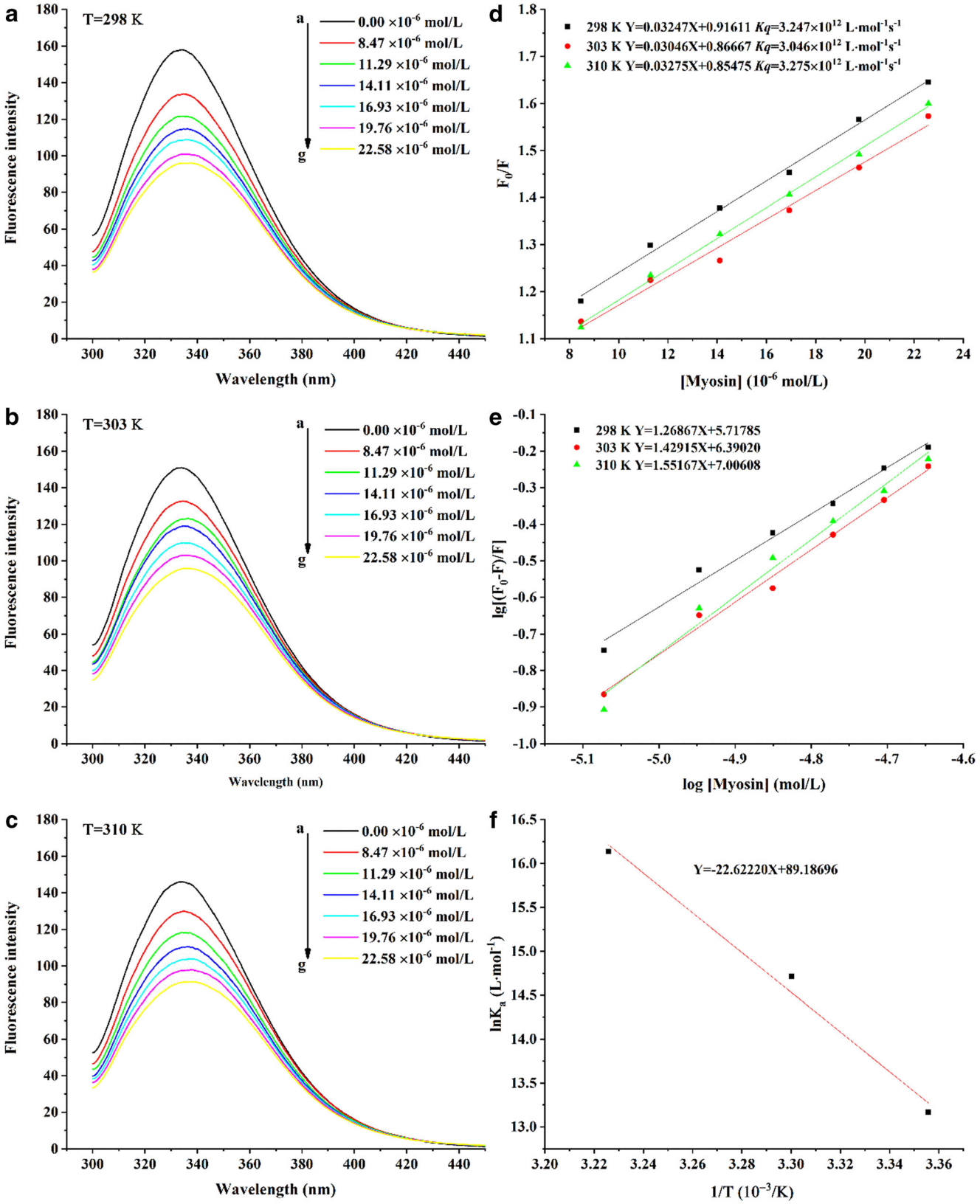

Fig. 1 The intrinsic fluorescence changes of myosin without or with different concentrations of CGA at 298 K (**a**), 303 K (**b**), and 310 K (**c**) (λ_{ex} = 280 nm). (**d**) The Stern-Volmer plots and the equation for the quenching of myosin by CGA in 298 K, 308 K, and 318 K, respectively. The plots for the static quenching of myosin by CGA (298 K, 308 K, and 318 K) (**e**). The Van't Hoff plot for the interaction of myosin and CGA. $C_{(myosin)}$ = 0.5 mg/mL; $C_{(CGA)}$ = 0 to 8 μg/mL (**f**)

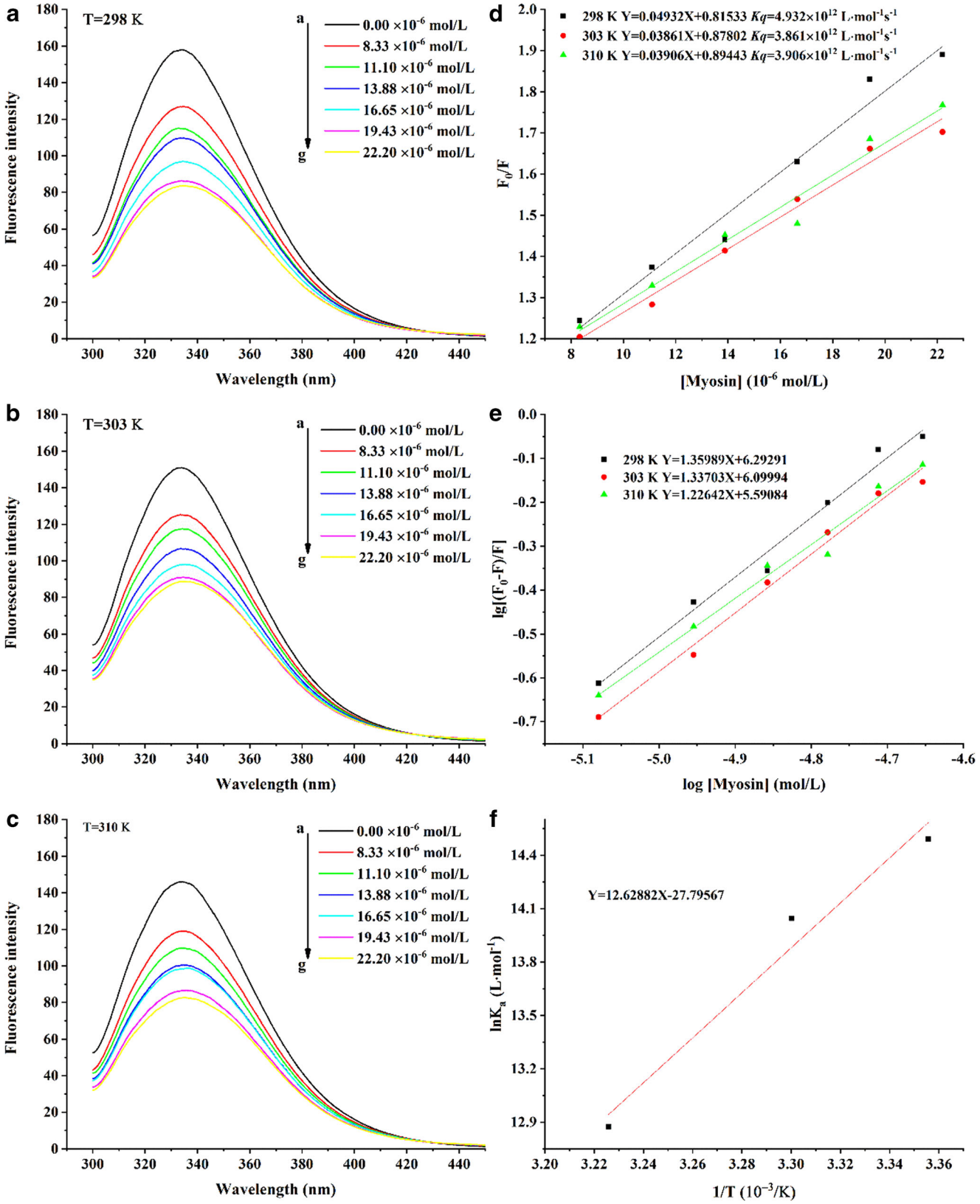

Fig. 2 The intrinsic fluorescence changes of myosin without or with different concentrations of RA at 298 K (**a**), 303 K (**b**), and 310 K (**c**) (λ_{ex} = 280 nm). (**d**) The Stern-Volmer plots and the equation for the quenching of myosin by RA in 298 K, 308 K, and 318 K, respectively. The plots for the static quenching of myosin by RA (298 K, 308 K, and 318 K) (**e**). The Van't Hoff plot for the interaction of myosin and RA. $C_{(myosin)}$ = 0.5 mg/mL; $C_{(RA)}$ = 0 to 8 μg/mL (**f**)

by 39.23% and 47.09% with the highest concentration of CGA and RA at 298 K, respectively. These results indicate that intrinsic fluorescence of myosin is quenched by CGA and RA as quenchers, and the quenching effect of RA is stronger than that of CGA. The reason could be the difference in molecular structures of RA and CGA (Hasni et al. 2011). From Fig. 1, it is clear that the emission peak of myosin changed slightly with the increase of CGA concentration, and the red shift increased with the rise in temperature. It is reported that the presence of anthocyanins in grape skins cause changes in the microenvironment of amino acids of whey protein isolates (Stănciuc et al. 2017). Thus, the binding of CGA is associated with the changes in the microenvironment of myosin which indicates that the tryptophan residue moved into a more hydrophilic environment with the addition of CGA (Kang et al. 2004).

The Fluorescence Quenching Mechanism

The addition of polyphenols leads to the quenching of myosin intrinsic fluorescence, and fluorescence data measured at various temperatures could be utilized to understand the corresponding quenching mechanism. Potential modes of fluorescence quenching include mainly dynamic quenching (caused by collision) and static quenching (caused by formation of stable complexes) (Ren et al. 2019). Figures 1 d and 2 d show the near linear plots for CGA-myosin and RA-myosin systems obtained at three different temperatures (298 K, 303 K, and 310 K) after analyzing the fluorescence quenching data according to the Stern-Volmer equation (Eq. (1)). It can be seen that the relationship between the values of F_0/F and myosin contents shows a good linear correlation at different temperatures as a correlated coefficient (R^2) as illustrated in Table 1. Dynamic quenching constant (K_{sv}) values were obtained from the slopes, whereas biomolecule quenching rate constant (K_q) values were calculated using Eq. (1). Obviously, K_q values are much higher than the maximum diffusion-limited quenching in water (2.0×10^{10} L mol^{-1} s^{-1}) which indicates that the quenching method is more likely to be static quenching than dynamic quenching (Cui et al. 2015). It suggests that both fluorescence quenching modes of CGA-myosin and RA-myosin systems are static quenching.

Analysis of the Binding Parameters

Assuming independent bindings of different polyphenols to binding sites on myosin, values of the binding constant (K_a) and binding sites (n) of CGA-myosin and RA-myosin interactions at various temperatures were obtained from fluorescence data using the double-logarithm equation (Eq. (2)). The plots of CGA and RA are shown in Figs. 1e and 2e, respectively. Values of K_a and n obtained for CGA-myosin and RA-myosin system were calculated and are summarized in Table 1. Both binding site numbers of CGA and RA were found to be close to 1.0, indicating the binding molar ratio of 1:1 between both polyphenols and myosin. The K_a values increased with rising temperature for CGA-myosin and decreased with rising temperature for RA-myosin systems, respectively. This indicates that the binding reactions of CGA-myosin and RA-myosin systems are endothermic and exothermic reactions, respectively. This conclusion can be well-explained by the changes in enthalpy (ΔH) displayed in Table 1. Furthermore, the K_a values decreased with increasing temperature indicating that the formation of polyphenol-myosin complex became more difficult, and there was a relative fall in the complex stability (Joye et al. 2015). Therefore, it is concluded that CGA-myosin complex was easily formed compared with that of RA-myosin complex and showed higher stability.

Thermodynamic Parameters Measurement

Thermodynamic measurements could be helpful in determining the major binding forces between polyphenols and myosin. In general, there are four major non-covalent binding forces between quencher and protein which include

Table 1 Quenching and binding constants, and relative thermodynamic parameters for the interaction of myosin with CGA/RA at different temperatures

Polyphenol	T (K)	K_{sv} (L·mol^{-1})	R^a	K_a (L·mol^{-1})	N	R^b	ΔG (kJ·mol^{-1})	ΔH (kJ·mol^{-1})	ΔS (kJ·mol^{-1}·K^{-1})	R^c
CGA	298	3.247×10^4	0.9979	5.222×10^5	1.269	0.9944	− 32.62	188.08	741.50	− 0.9939
	303	3.046×10^4	0.9933	2.456×10^6	1.429	0.9956	− 37.07			
	310	3.275×10^4	0.9988	1.014×10^7	1.552	0.9919	− 41.58			
RA	298	4.932×10^4	0.9885	1.963×10^6	1.360	0.9924	− 35.90	− 105.00	− 231.10	0.9857
	303	3.861×10^4	0.9924	1.259×10^6	1.337	0.9944	− 35.38			
	310	3.906×10^4	0.9866	3.898×10^5	1.226	0.9909	− 33.18			

R^a is the correlated coefficient of the Stern-Volmer equation. R^b is the correlated coefficient of the equation of K_a and n. R^c is the correlated coefficient of the Van't Hoff equation

hydrophobic interactions, hydrogen bonding, van der Waals forces, and electrostatic interactions (Jia et al. 2017). The thermodynamic parameters, such as enthalpy change (ΔH), entropy change (ΔS), and free energy change (ΔG), are dependent on temperature, which can be determined in order to specify the non-covalent acting forces between polyphenols and myosin. The ΔH and ΔS for the interaction between polyphenols and myosin were calculated by Eq. (3) and the ΔG obtained using the Gibbs-Helmholtz Eq. (4). The corresponding results are shown in Figs. 1f, 2f, and Table 1. For ligand–protein interaction, $\Delta H > 0$, $\Delta S > 0$ represent hydrophobic interaction; $\Delta H < 0$, $\Delta S < 0$ exhibit hydrogen bonds and Vander Waals' interactions; $\Delta H < 0$, $\Delta S > 0$ signify electrostatic forces (Ross and Subramanian 1981). Negative ΔG (Table 1) indicates that the process of myosin combination with polyphenols was spontaneous. From Table 1, the negative values of ΔH and ΔS indicate that the binding forces between RA and myosin were mainly hydrogen bonds and vander Waals' interactions. On the contrary, the positive values of ΔH and ΔS indicate that the hydrophobic interaction contributed significantly to the interaction of CGA and myosin. However, some reports have suggested that the interaction between RA and human serum albumin is mainly hydrophobic interaction (Peng et al. 2016). Some researchers have found that hydrogen bonds and van der Waals force promote the combination of CGA and β-lactoglobulin (Jia et al. 2017). These reports assert that different binding forces are involved in the binding of polyphenols and different proteins. In future research, with the development of the optimized myosin molecule structure, the interaction between polyphenols and myosin could be predicted with the use of molecular simulation technologies.

Synchronous Fluorescence Spectral Measurement

The synchronous fluorescence spectra can provide the information concerning the microenvironmental changes of chromophore molecules in protein before and after binding with polyphenols. When the wavelength intervals ($\Delta\lambda = \lambda em - \lambda ex$) are set at 15 nm and 60 nm, synchronous fluorescence spectra offer the characteristic information of tyrosine (Tyr) and tryptophan (Trp) residues, respectively (Azimi et al. 2011). The synchronous fluorescence spectra of CGA-myosin and RA-myosin at room temperature are shown in Fig. 3. The results show that the fluorescence intensity of Tyr and Trp decreased significantly with increasing polyphenol concentration. Moreover, the fluorescence intensities of Trp residues were higher than those of Tyr residues. This phenomenon is not affected by changes in the types and concentrations of polyphenols indicating that Trp residues contribute more to the fluorescence generation of myosin than Tyr residue. Additionally, there was no visible change in the position of the maximum emission wavelength of Trp residues (Fig. 3 a2 and b2); however, there appeared to be a slightly blue shift for that of Tyr residues (CGA-myosin, from 286.40 to 285.80 nm; RA-myosin, from 286.40 to 285.80 nm) (Fig. 3 a1 and b1) indicating a slight change in the microenvironment near the tyrosine residue (Yuan et al. 2007).

Circular Dichroism Spectra

Circular dichroism (CD) spectroscopy is an important method for studying the conformation changes of protein, especially the secondary structure (Whitmore and Wallace 2008). The CD spectra of myosin and polyphenol-myosin complexes are shown in Fig. 4. The two negative peaks appeared at 208 nm and 222 nm within the detected wavelength range (200 to 240 nm) which are mainly attributed to the contribution of α-helix of protein, and the results of α-helix content are also presented in Fig. 4 (Yang et al. 1986). It is clear to see that the α-helix content of polyphenol-myosin complexes increased to 50.4% or 55.00% from the initial 48.00%, when CGA and RA were added into myosin solutions, respectively. The increase in the α-helix content of polyphenol-myosin complexes illustrates that the binding of CGA or RA to myosin enhanced the degree of the shrinking of the myosin skeleton which has already been reported by other researchers (Tang et al. 2014). In addition, the change of the α-helix of proteins can be attributed to hydrogen bonding or hydrophobic interaction (Li et al. 2009) contributing to the binding of RA or CGA with myosin, respectively.

UV Absorption Spectra Measurement

UV absorption spectroscopy is a simple way to study the tertiary structural changes of myosin before and after adding different concentrations of CGA and RA (Lange and Balny 2002). UV absorption spectra of myosin and myosin-polyphenol systems are presented in Fig. 5a1, b1. The UV absorption spectral intensity of polyphenols under experimental conditions is negligible (data not shown). The absorbance peak at 275 nm is the featured absorption peak of aromatic amino acid (Tyr and Trp) residues, and the UV absorbance values of myosin gradually increased with the addition of CGA or RA, respectively. In addition, the absorbance peak of myosin at 275 nm showed a slight red shift with increasing polyphenol concentrations indicating that CGA or RA has no significant effect on aromatic amino acids.

In order to provide detailed information of aromatic amino acids (especially Trp and Tyr), UV absorption spectrum was analyzed utilizing the second derivative. UV second derivative absorption spectra were used because they can provide the exact qualitative and quantitative information from uncertain band spectra (Rojas et al. 1988). The second derivative absorption spectra from 280 to 310 nm of myosin samples are presented in Fig. 5 a2 and b2. Compared with the original UV

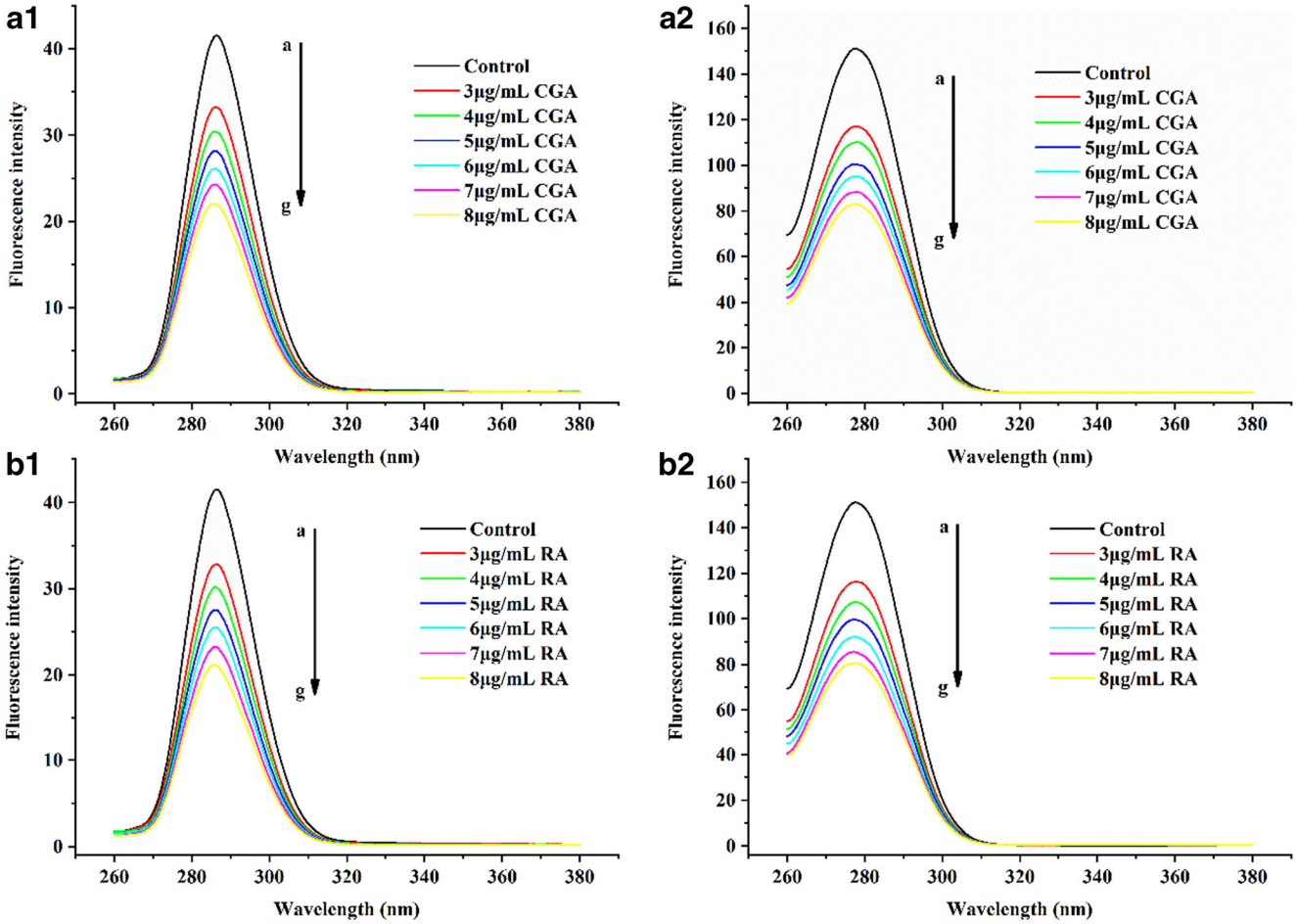

Fig. 3 Synchronous fluorescence spectra of the interaction between myosin and CGA (**a**)/RA (**b**) (0 to 8 μg/mL) at $\Delta\lambda = 15$ nm (**a1**, and **b1**) and at $\Delta\lambda = 60$ nm (**a2**, and **b2**); $C_{(\text{myosin})} = 0.5$ mg/mL; the experiment was carried out at room temperature

spectra, the UV second derivative absorption spectra have two distinct troughs (284 nm, 291 nm) and peaks (288 nm, 295 nm) from 280 to 310 nm, respectively. In addition, peaks at 288 nm belong to Trp and Tyr residues, and the peaks at 295 nm are attributed to Trp residues (Wang et al. 2018). When adding the polyphenols, the peaks at 288 nm displayed almost no change; however, the other peaks showed a slight red shift shifting from 295 to 296 nm, which indicates that Trp residues were exposed to a more hydrophilic environment.

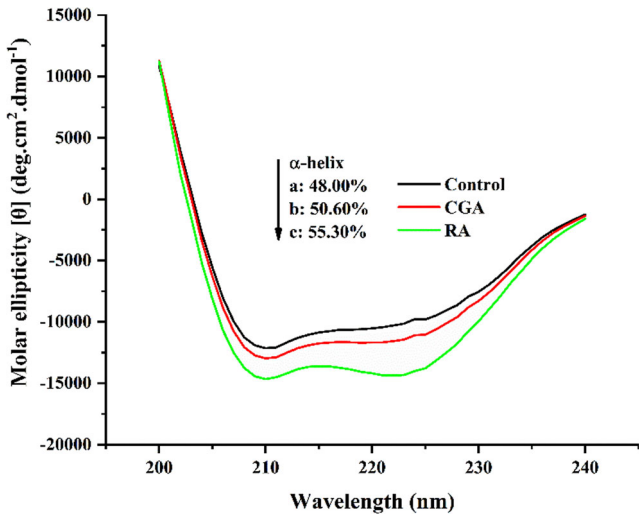

Fig. 4 CD spectra of myosin (curve a), CGA-myosin (curve b), and RA-myosin (curve c). $C_{\text{myosin}} = 0.05$ mg/mL, $C_{(\text{CGA})} = C_{(\text{RA})} = 0.8$ μg/mL

Furthermore, the relative amounts and three-dimensional positions of Trp and Tyr can be characterized by the peak-to-trough ratio (*r*) (Lange and Balny 2002). The "*r*" value is calculated by "*a*" and "*b*" which represents the peak-to-trough values (284 to 288 nm; 291 to 295 nm), respectively. In general, the higher the "*r*" values, the greater the Tyr residues exposed to the solution which are related to the strength of polarity (Saleem and Ahmad 2016). Figure 5 a2, b2 shows that the "*r*" values respectively increased to 2.58 and 2.61 for CGA-myosin and RA-myosin systems compared with that of the original myosin 2.23. This finding indicates that more Tyr residues of myosin induced an increase in polarity in the microenvironment after the addition of CGA and RA. Meanwhile, the "*r*" value of RA-myosin systems was slightly higher than that of the CGA-myosin system which indicates that RA is more likely to expose Tyr residues to a solution than CGA. Moreover, the exposure of more Tyr residues

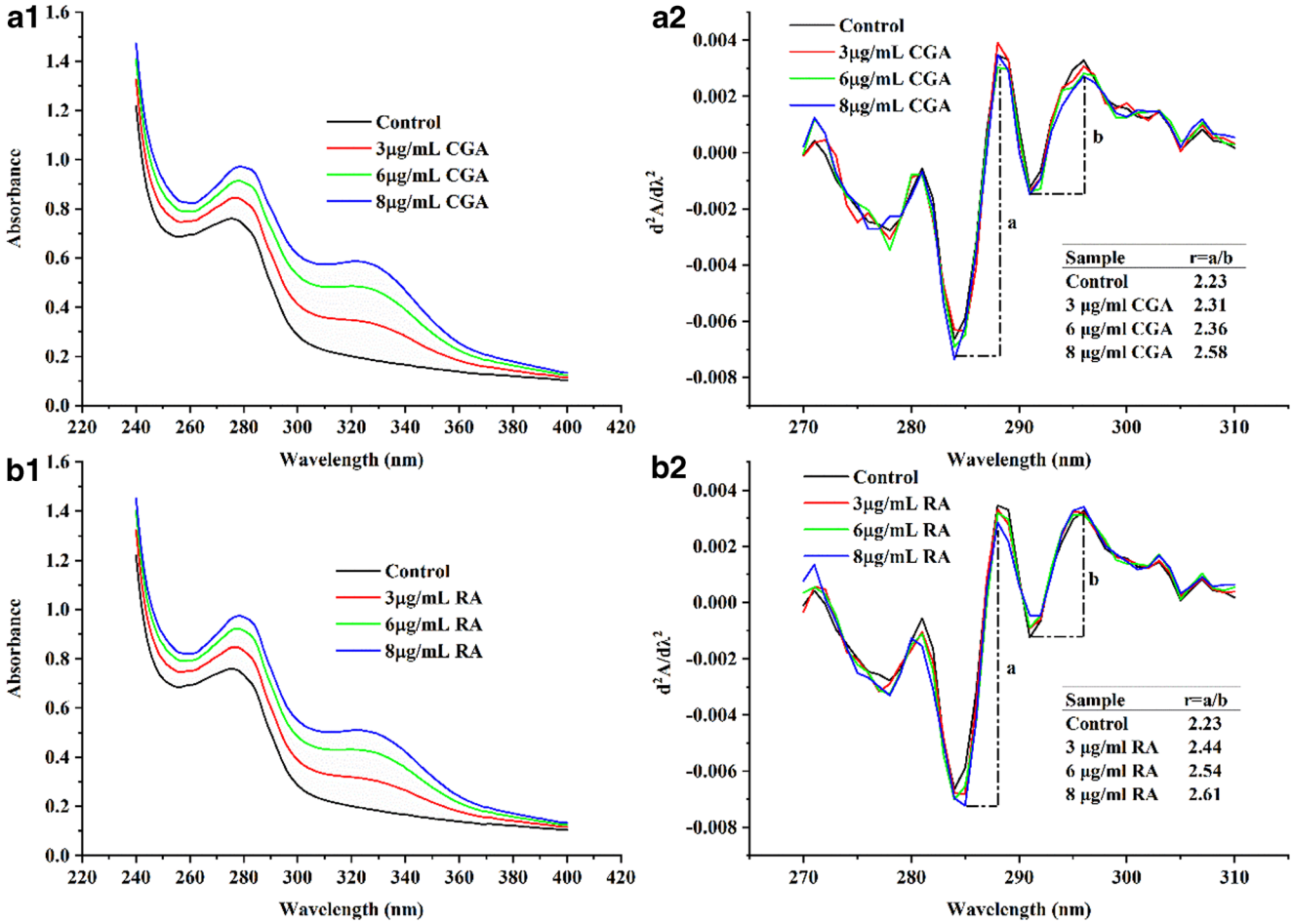

Fig. 5 Zero-order UV absorption spectra (**a1**, **b1**) and second derivative UV absorption spectra of myosin (**a2**, **b2**) (0.5 mg/mL) added with CGA/RA (0, 3, 6 and 8 μg/mL). The letters "**a**" and "**b**" represent the peak-to-trough values for the two main peaks. The ratio (r = a/b) of the peak-to-trough values in the second derivative spectra of myosin with different CGA/RA concentrations are summarized in the table

could reduce the surface hydrophobicity of myosin since Tyr is a kind of hydrophilic or polar amino acid.

Turbidity Measurement

The turbidity produced after the interaction between protein and polyphenol depends on the concentration and ratio of protein and polyphenol, and is also closely related to the type of polyphenols (Siebert et al. 1996). The turbidity of myosin before and after the addition of polyphenols is determined by the magnitude of turbidity (Yongsawatdigul and Sinsuwan 2007). The results of different systems are shown in Fig. 6. From Fig. 6, it can clearly be seen that the turbidity of myosin increased after the addition of polyphenols. However, it seems that CGA caused higher turbidity levels of myosin growth compared with RA which may in turn depend on the different binding modes of RA and CGA. The turbidity is influenced by the scale of the binding forces and the number of possible binding sites of polyphenols (Siebert et al. 1996).

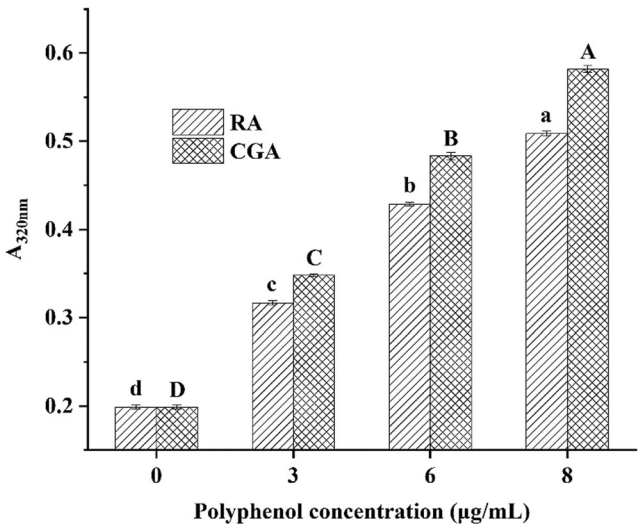

Fig. 6 Turbidity (A_{320nm}) of myosin (0.5 mg/mL) added with CGA/RA (0, 3, 6 and 8 μg/mL). Different lower case letters indicate significant differences in turbidity values of myosin and myosin-RA complexes ($p < 0.05$). Different capital letters indicate significant differences in turbidity values of myosin and myosin-CGA complexes ($p < 0.05$)

Surface Hydrophobicity Measurement

It has been reported that the change in surface hydrophobicity may be due to the ligand inserted into the hydrophobic surface of the protein (Xu et al. 2015), and the interaction between polyphenols and proteins could change the conformation of the protein. ANS works as a hydrophobic fluorescent probe and has been widely used to study protein conformational changes (Cao et al. 2015). The changes in S_0-ANS before and after adding polyphenols into myosin are shown in Fig. 7. It can be noted that the surface hydrophobicity of myosin shows a decreasing trend with the addition of polyphenols, and the surface hydrophobicity of the RA-myosin system was lower than that of the CGA-myosin system under the same concentration of polyphenol. This indicates that RA has higher capacity to increase the polarity of the surrounding solution than CGA which is similar to the results of a previous study (Jia et al. 2017). This conclusion is in good agreement with the results of CD spectra and UV absorption spectra.

Particle Size Measurement

The dynamic light scattering (DLS) is used to identify the particle size of myosin and polyphenol-myosin complexes for evaluating the myosin aggregation in order to investigate the binding of the complex. DLS can monitor the dissociation or monomer aggregation of myosin filaments by measuring the hydrodynamic diameter of the particles in solution. The molecular weight distribution curve (intensity %), polydispersity index (PDI), and Z-average (d.nm) of myosin and myosin-polyphenol systems are presented in Fig. 8. From Fig. 8, it can be observed that the PDI and Z-average values of myosin alone are 0.252 and 270.3, respectively. However, after the addition of polyphenols, the values of PDI and Z-average increased to 0.256, 281.4, and 0.352, 360.4 for myosin-RA and myosin-CGA systems, respectively. This indicates that polyphenols could promote the aggregation of myosin and reduce the dispersion of myosin. The other explanation is that during the addition, polyphenols were attached to the surface of proteins by cross-linking different proteins and induced the production of dimerization, which resulted in increasing the insolubility and particle size (Jöbstl et al. 2004). This result is in good agreement with the results of turbidity. At the same time, a similar phenomenon was reported in a study of the interaction between zein nanoparticles and quercetagetin which showed a narrower size distribution of zein (Sun et al. 2016; Sui et al. 2018)

Determination of Reactive Sulfhydryl Groups

The reactive SH group is a key active group in the tertiary conformational changes of proteins. As shown in Fig. 9, the contents of reactive SH groups for myosin and myosin-polyphenol systems were investigated. After the addition of CGA and RA (8 μg/mL), the reactive sulfhydryl group contents of myosin-CGA and myosin-RA systems rose to 9.78 and 9.40 nmol/mg of protein from the original value of 8.79 nmol/mg of protein, respectively. From Fig. 9, it can clearly be seen that the reactive sulfhydryl group content of myosin was significantly positively correlated to the concentration of polyphenols ($p < 0.05$). Moreover, the myosin-CGA system had higher reactive sulfhydryl group content than that of the myosin-RA system. It has been reported that

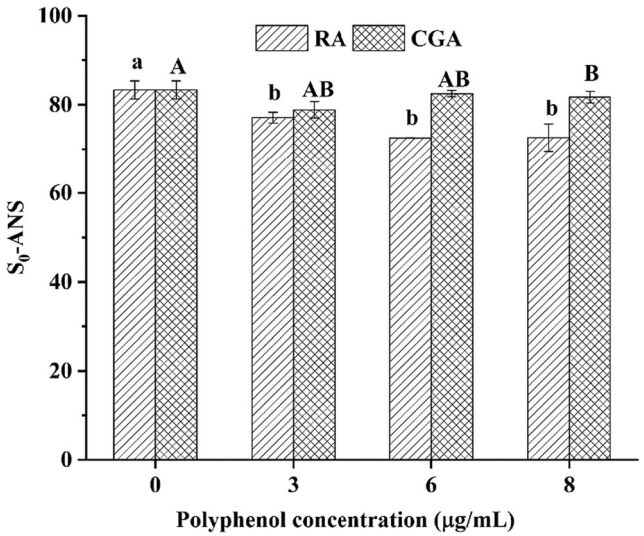

Fig. 7 Effects of different CGA/RA concentrations (0, 3, 6, and 8 μg/mL) on surface hydrophobicity (S_0-ANS) of myosin (0.5 mg/mL). Different lower case letters indicate significant differences in S_0-ANS values of myosin and myosin-RA complexes ($p < 0.05$). Different capital letters indicate significant differences in S_0-ANS values of myosin and myosin-CGA complexes ($p < 0.05$)

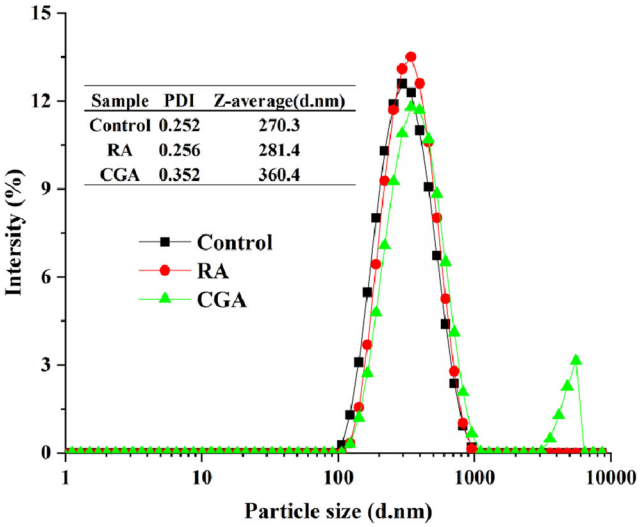

Fig. 8 Particle size distribution (intensity %) of myosin, myosin-RA, and myosin-CGA complex. The polydispersity index (PDI) and Z-average (d.nm) values of myosin, myosin-RA, and myosin-CGA complex are summarized in the Table. $C_{(myosin)} = 0.5$ mg/mL, $C_{(CGA)} = C_{(RA)} = 8$ μg/mL

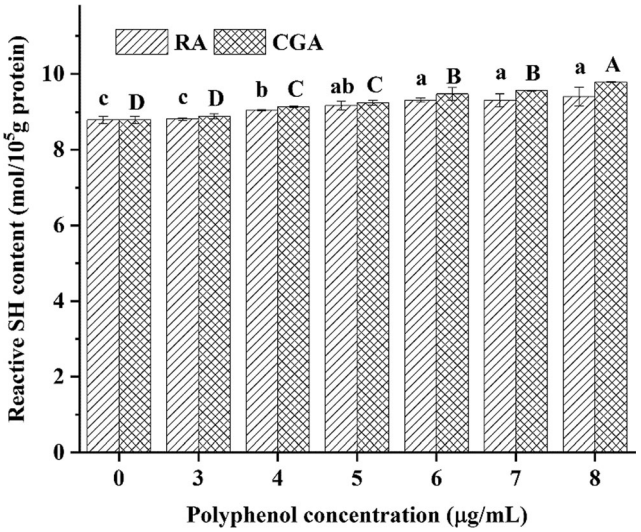

Fig. 9 Effects of different CGA/RA concentrations (0, 3, 4, 5, 6, 7, and 8 μg/mL) on reactive SH of myosin (0.5 mg/mL). Different lower case letters indicate significant differences in reactive SH values of myosin and myosin-RA complexes ($p < 0.05$). Different capital letters indicate significant differences in reactive SH values of myosin and myosin-CGA complexes ($p < 0.05$)

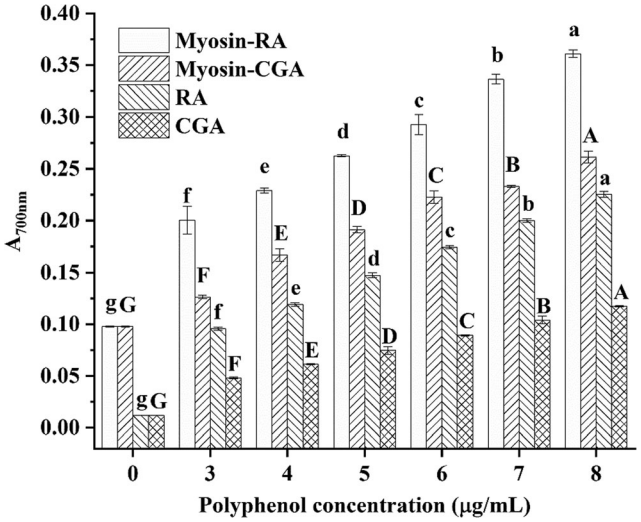

Fig. 10 Reducing power (A_{700nm}) of different CGA/RA concentrations (0, 3, 4, 5, 6, 7, and 8 μg/mL) with and without myosin (0.5 mg/mL). Different lower case letters indicate significant differences in reducing power values between different RA concentrations ($p < 0.05$). Different capital letters indicate significant differences in reducing power values between different CGA concentrations ($p < 0.05$)

polyphenol with special structure of gallate moiety induces the content of protein thiols and remains unchanged or decreased, resulting in the aggregation of proteins (Chen et al. 2011; Ishii et al. 2009). Both CGA and RA do not react to the thiol group of proteins due to lack of the typical structure of gallate moiety. On the contrary, it can increase the reactive sulfhydryl group content of myosin through protecting the myosin thiols.

Reducing Power Measurement

The reducing power test is considered to be the best method for assessing the electron donor capacity of antioxidants (Peng et al. 2010). The antioxidant activity of myosin binding to different polyphenols is evaluated by reducing the power assay. As depicted in Fig. 10, it was observed that the antioxidant capacities of myosin-polyphenol systems are higher than myosin, and these are significantly positively correlated to the concentration of polyphenols ($p < 0.05$). An interesting result found that myosin also has good reducing power and showed stronger reducing power due to a synergistic effect when it binds to polyphenols. A similar conclusion was also drawn that the formation of complexes β-cyclodextrins-CGA and α-tocopherol-RA further strengthened the reducing power of complexes (Shao et al. 2014; Panya et al. 2012). The oxidation products of polyphenols might be responsible for this synergistic interaction.

Furthermore, the antioxidant capacity of the myosin-RA system was found to be stronger than that of the myosin-CGA system at the same concentration. The difference in reducing power of two types of polyphenols could be related to their different structural formulas and hydroxyl activities. In addition, it was found that protein can maintain the stability of small organic molecules, which could explain the synergy between protein and polyphenols (Silva et al. 2018).

Conclusions

In the present study, multi-spectroscopic techniques were used to explore the interaction between polyphenols (CGA and RA) and grass carp myosin. Results show that both CGA and RA had great influence on intrinsic fluorescence, surface hydrophobicity, UV absorption intensity, turbidity, and alpha-helix of myosin, which are indicative of the types of interactions between polyphenols and myosin. Moreover, the analysis of the fluorescence quenching data shows that the binding process of the complex is spontaneous. The main interaction forces between RA and myosin are hydrogen bonding and van der Waals force; however, the hydrophobic interaction is the major interaction force between CGA and myosin. CGA and RA had the effect of protecting myosin sulfhydryl groups which reduced the degree of myosin oxidation. Moreover, the complexes of myosin and polyphenols exhibited the strongest synergistic antioxidant properties than any one of them. Thus, the present study can partly provide some insights into our understanding of the mechanism involved in the application of polyphenols in the preservation of aquatic products.

Funding Information This study was supported by the Nature Science Foundation of China (No. 31772047), the Fundamental Research Funds for the Central Universities (No. 2662019PY031), Chinese Ministry of Science and Technology (2019YFC1606003), and the China Agriculture Research System (CARS-45-27).

Compliance with Ethical Standards

Conflict of Interest The authors declare that they have no conflict of interest.

References

Azimi, O., Emami, Z., Salari, H., & Chamani, J. (2011). Probing the interaction of human serum albumin with norfloxacin in the presence of high-frequency electromagnetic fields: Fluorescence spectroscopy and circular dichroism investigations. *Molecules., 16*(12), 9792–9818.

Cao, L., Su, S., Regenstein, J. M., Xiong, S., & Liu, R. (2015). Ca2+-Induced conformational changes of myosin from silver carp (Hypophthalmichthys molitrix) in gelation. *Food Biophysics, 10*(4), 447–455.

Cao, Q., Du, H., Huang, Y., Hu, Y., You, J., Liu, R., Xiong, S., & Manyande, A. (2019). The inhibitory effect of chlorogenic acid on lipid oxidation of grass carp (Ctenopharyngodon idellus) during chilled storage. *Food and Bioprocess Technology., 12*(12), 2050–2061.

Chen, R., Wang, J.-B., Zhang, X.-Q., Ren, J., & Zeng, C.-M. (2011). Green tea polyphenol epigallocatechin-3-gallate (EGCG) induced intermolecular cross-linking of membrane proteins. *Archives of Biochemistry and Biophysics., 507*(2), 343–349.

Cui, Y., Liang, G., Hu, Y.-H., Shi, Y., Cai, Y.-X., Gao, H.-J., Chen, Q.-X., & Wang, Q. (2015). Alpha-substituted derivatives of cinnamaldehyde as tyrosinase inhibitors: Inhibitory mechanism and molecular analysis. *Journal of Agricultural and Food Chemistry., 63*(2), 716–722.

Dai, T., Chen, J., Li, Q., Li, P., Hu, P., Liu, C., & Li, T. (2018). Investigation the interaction between procyanidin dimer and α-amylase: Spectroscopic analyses and molecular docking simulation. *International Journal of Biological Macromolecules., 113*, 427–433.

Dan, Q., Xiong, W., Liang, H., Wu, D., Zhan, F., Chen, Y., Ding, S., & Li, B. (2019). Characteristic of interaction mechanism between β-lactoglobulin and nobiletin: A multi-spectroscopic, thermodynamics methods and docking study. *Food Research International., 120*, 255–263.

Daskalova, A. (2019). Farmed fish welfare: Stress, post-mortem muscle metabolism, and stress-related meat quality changes. *International Aquatic Research., 11*(2), 113–124.

Fan, W., Chi, Y., & Zhang, S. (2008). The use of a tea polyphenol dip to extend the shelf life of silver carp (Hypophthalmicthys molitrix) during storage in ice. *Food Chemistry., 108*(1), 148–153.

Feng, X., Ng, V. K., Mikš-Krajnik, M., & Yang, H. (2017). Effects of fish gelatin and tea polyphenol coating on the spoilage and degradation of myofibril in fish fillet during cold storage. *Food and Bioprocess Technology., 10*(1), 89–102.

Hasni, I., Bourassa, P., Hamdani, S., Samson, G., Carpentier, R., & Tajmir-Riahi, H.-A. (2011). Interaction of milk α- and β-caseins with tea polyphenols. *Food Chemistry., 126*(2), 630–639.

Hosseini, S. F., Rezaei, M., Zandi, M., & Ghavi, F. F. (2016). Effect of fish gelatin coating enriched with oregano essential oil on the quality of refrigerated rainbow trout fillet. *Journal of Aquatic Food Product Technology., 25*(6), 835–842.

Ishii, T., Ishikawa, M., Miyoshi, N., Yasunaga, M., Akagawa, M., Uchida, K., & Nakamura, Y. (2009). Catechol type polyphenol is a potential modifier of protein sulfhydryls: Development and application of a new probe for understanding the dietary polyphenol actions. *Chemical Research in Toxicology., 22*(10), 1689–1698.

Jia, J., Gao, X., Hao, M., & Tang, L. (2017). Comparison of binding interaction between β-lactoglobulin and three common polyphenols using multi-spectroscopy and modeling methods. *Food Chemistry., 228*, 143–151.

Jiang, L., & Wu, S. (2018). Pullulan suppresses the denaturation of myofibrillar protein of grass carp (Ctenopharyngodon idella) during frozen storage. *International Journal of Biological Macromolecules., 112*, 1171–1174.

Jiang, J., Zhang, Z., Zhao, J., & Liu, Y. (2018). The effect of non-covalent interaction of chlorogenic acid with whey protein and casein on physicochemical and radical-scavenging activity of in vitro protein digests. *Food Chemistry., 268*, 334–341.

Jöbstl, E., O'Connell, J., Fairclough, J. P. A., & Williamson, M. P. (2004). Molecular model for astringency produced by polyphenol/protein interactions. *Biomacromolecules., 5*(3), 942–949.

Joye, I. J., Davidov-Pardo, G., Ludescher, R. D., & McClements, D. J. (2015). Fluorescence quenching study of resveratrol binding to zein and gliadin: Towards a more rational approach to resveratrol encapsulation using water-insoluble proteins. *Food Chemistry., 185*, 261–267.

Kang, J., Liu, Y., Xie, M.-X., Li, S., Jiang, M., & Wang, Y.-D. (2004). Interactions of human serum albumin with chlorogenic acid and ferulic acid. *Biochimica et Biophysica Acta (BBA) - General Subjects., 1674*(2), 205–214.

Karaca, A. C., Low, N., & Nickerson, M. (2011). Emulsifying properties of chickpea, faba bean, lentil and pea proteins produced by isoelectric precipitation and salt extraction. *Food Research International., 44*(9), 2742–2750.

Kominz, D. R., Hough, A., Symonds, P., & Laki, K. (1954). The amino acid composition of actin, myosin, tropomyosin and the meromyosins. *Archives of Biochemistry and Biophysics., 50*(1), 148–159.

Lakowicz, J. (1999). *Principles of fluorescence spectroscopy (2nd ed)*. New York: Kluwer/Plenum. https://doi.org/10.1007/978-0-387-46312-4.

Lange, R., & Balny, C. (2002). UV-visible derivative spectroscopy under high pressure. *Biochimica et Biophysica Acta (BBA) - Protein Structure and Molecular Enzymology., 1595*(1), 80–93.

Li, Y., Lim, L. T., & Kakuda, Y. (2009). Electrospun zein fibers as carriers to stabilize (-)-epigallocatechin gallate. *Journal of Food Science, 74*(3), C233–C240.

Li, T., Hu, P., Dai, T., Li, P., Ye, X., Chen, J., & Liu, C. (2018). Comparing the binding interaction between β-lactoglobulin and flavonoids with different structure by multi-spectroscopy analysis and molecular docking. *Spectrochimica Acta Part A: Molecular and Biomolecular Spectroscopy., 201*, 197–206.

Liu, R., Zhao, S.-M., Xie, B.-J., & Xiong, S.-B. (2011). Contribution of protein conformation and intermolecular bonds to fish and pork gelation properties. *Food Hydrocolloids, 25*(5), 898–906.

Lowry, O. H., Rosebrough, N. J., Farr, A. L., & Randall, R. J. (1951). Protein measurement with the Folin phenol reagent. *Journal of Biological Chemistry., 193*(1), 265–275.

Luan, L., Fu, S., Yuan, C., Ishimura, G., Chen, S., Chen, J., & Hu, Y. (2017). Combined effect of superchilling and tea polyphenols on the preservation quality of hairtail (Trichiurus haumela). *International Journal of Food Properties, 20*(sup1), S992–S1001.

Mohammadian, M., & Madadlou, A. (2016). Characterization of fibrillated antioxidant whey protein hydrolysate and comparison with fibrillated protein solution. *Food Hydrocolloids, 52*, 221–230.

Ojagh, S. M., Rezaei, M., & Razavi, S. H. (2014). Improvement of the storage quality of frozen rainbow trout by chitosan coating incorporated with cinnamon oil. *Journal of Aquatic Food Product Technology., 23*(2), 146–154.

Panya, A., Kittipongpittaya, K., Laguerre, M., Bayrasy, C., Lecomte, J., Villeneuve, P., McClements, D. J., & Decker, E. A. (2012). Interactions between α-tocopherol and rosmarinic acid and its alkyl esters in emulsions: Synergistic, additive, or antagonistic effect?

Journal of Agricultural and Food Chemistry., 60(41), 10320–10330.

Park, J. W., & Lanier, T. C. (1989). Scanning calorimetric behavior of tilapia myosin and actin due to processing of muscle and protein purification. *Journal of Food Science., 54*(1), 49–51.

Peng, X., Kong, B., Xia, X., & Liu, Q. (2010). Reducing and radical-scavenging activities of whey protein hydrolysates prepared with Alcalase. *International Dairy Journal., 20*(5), 360–365.

Peng, X., Wang, X., Qi, W., Su, R., & He, Z. (2016). Affinity of rosmarinic acid to human serum albumin and its effect on protein conformation stability. *Food Chemistry., 192*, 178–187.

Peng, X., Wang, Y., Xing, J., Wang, R., Shi, X., & Guo, S. (2017). Characterization of particles in soymilks prepared by blanching soybeans and traditional method: A comparative study focusing on lipid-protein interaction. *Food Hydrocolloids, 63*, 1–7.

Qiu, X., Chen, S., Liu, G., & Yang, Q. (2014). Quality enhancement in the Japanese sea bass (Lateolabrax japonicas) fillets stored at 4°C by chitosan coating incorporated with citric acid or licorice extract. *Food Chemistry., 162*, 156–160.

Reesha, K. V., Panda, S. K., Bindu, J., & Varghese, T. O. (2015). Development and characterization of an LDPE/chitosan composite antimicrobial film for chilled fish storage. *International Journal of Biological Macromolecules., 79*, 934–942.

Ren, C., Xiong, W., Li, J., & Li, B. (2019). Comparison of binding interactions of cyanidin-3-O-glucoside to β-conglycinin and glycinin using multi-spectroscopic and thermodynamic methods. *Food Hydrocolloids, 92*, 155–162.

Rodríguez, A., Cruz, J. M., Paseiro-Losada, P., & Aubourg, S. P. (2012). Effect of a polyphenol–vacuum packaging on lipid deterioration during an 18-month frozen storage of coho salmon (Oncorhynchus kisutch). *Food and Bioprocess Technology., 5*(6), 2602–2611.

Rojas, F. S., Ojeda, C. B., & Pavon, J. M. C. (1988). Derivative ultraviolet—Visible region absorption spectrophotometry and its analytical applications. *Talanta., 35*(10), 753–761.

Ross, P. D., & Subramanian, S. (1981). Thermodynamics of protein association reactions: Forces contributing to stability. *Biochemistry., 20*(11), 3096–3102.

Saleem. R., & Ahmad, R. (2016). Effect of low frequency ultrasonication on biochemical and structural properties of chicken actomyosin. Food Chemistry. 205, 43–51.

Shao, P., Zhang, J., Fang, Z., & Sun, P. (2014). Complexing of chlorogenic acid with β-cyclodextrins: Inclusion effects, antioxidative properties and potential application in grape juice. *Food Hydrocolloids, 41*, 132–139.

Siebert, K. J., Troukhanova, N. V., & Lynn, P. Y. (1996). Nature of polyphenol−protein interactions. *Journal of Agricultural and Food Chemistry., 44*(1), 80–85.

Silva, C. E. L., Hudson, E. A., Agudelo, Á. J. P., da Silva, L. H. M., Pinto, M. S., do Carmo Hespanhol, M., Barros, F. A. R., & dos Santos Pires, A. C. (2018). β-Carotene and milk protein complexation: A thermodynamic approach and a photo stabilization study. *Food and Bioprocess Technology., 11*(3), 610–620.

Stănciuc, N., Turturică, M., Oancea, A. M., Barbu, V., Ioniță, E., Aprodu, I., & Râpeanu, G. (2017). Microencapsulation of anthocyanins from grape skins by whey protein isolates and different polymers. *Food and Bioprocess Technology., 10*(9), 1715–1726.

Sui, X., Sun, H., Qi, B., Zhang, M., Li, Y., & Jiang, L. (2018). Functional and conformational changes to soy proteins accompanying anthocyanins: Focus on covalent and non-covalent interactions. *Food Chemistry., 245*, 871–878.

Sun, C., Yang, J., Liu, F., Yang, W., Yuan, F., & Gao, Y. (2016). Effects of dynamic high-pressure microfluidization treatment and the presence of quercetagetin on the physical, structural, thermal, and morphological characteristics of zein nanoparticles. *Food and Bioprocess Technology., 9*(2), 320–330.

Sun, L., Sun, J., Liu, D., Fu, M., Yang, X., & Guo, Y. (2018). The preservative effects of chitosan film incorporated with thinned young apple polyphenols on the quality of grass carp (Ctenopharyngodon idellus) fillets during cold storage: Correlation between the preservative effects and the active properties of the film. *Food Packaging and Shelf Life., 17*, 1–10.

Tang, L., Zuo, H., & Shu, L. (2014). Comparison of the interaction between three anthocyanins and human serum albumins by spectroscopy. *Journal of Luminescence., 153*, 54–63.

Wang, T., Li, Z., Yuan, F., Lin, H., & Pavase, T. R. (2017). Effects of brown seaweed polyphenols, alpha-tocopherol, and ascorbic acid on protein oxidation and textural properties of fish mince (Pagrosomus major) during frozen storage. *Journal of the Science of Food and Agriculture, 97*(4), 1102–1107.

Wang, G., Liu, M., Cao, L., Yongsawatdigul, J., Xiong, S., & Liu, R. (2018). Effects of different NaCl concentrations on self-assembly of silver carp myosin. *Food Bioscience, 24*, 1–8.

Whitmore, L., & Wallace, B. A. (2008). Protein secondary structure analyses from circular dichroism spectroscopy: Methods and reference databases. *Biopolymers., 89*(5), 392–400.

Wu, C., Fu, S., Xiang, Y., Yuan, C., Hu, Y., Chen, S., Liu, D., & Ye, X. (2016). Effect of chitosan gallate coating on the quality maintenance of refrigerated (4 °C) silver pomfret (Pampus argentus). *Food and Bioprocess Technology., 9*(11), 1835–1843.

Wu, M., Li, C., Du, W., Yang, X., & Liu, Z. (2018). Preparation of chitosan/rosemary extract nanoparticles and their application for inhibiting lipid oxidation in grass carp (Ctenopharyngodon idellus) during cold storage. *Journal of Aquatic Food Product Technology., 27*(6), 759–770.

Xu, X., Liu, W., Zhong, J., Luo, L., Liu, C., Luo, S., & Chen, L. (2015). Binding interaction between rice glutelin and amylose: Hydrophobic interaction and conformational changes. *International Journal of Biological Macromolecules., 81*, 942–950.

Xu, H., Lu, Y., Zhang, T., Liu, K., Liu, L., He, Z., Xu, B., & Wu, X. (2019). Characterization of binding interactions of anthraquinones and bovine β-lactoglobulin. *Food Chemistry., 281*, 28–35.

Yan, X., Liu, B., Chong, B., & Cao, S. (2013). Interaction of Cefpiramide sodium with bovine hemoglobin and effect of the coexistent metal ion on the protein-drug association. *Journal of Luminescence., 142*, 155–162.

Yang, J. T., Wu, C.-S. C., & Martinez, H. M. (1986). [11] Calculation of protein conformation from circular dichroism. In *Methods in enzymology* (Vol. 130, pp. 208–269). Academic press.

Yongsawatdigul, J., & Sinsuwan, S. (2007). Aggregation and conformational changes of tilapia actomyosin as affected by calcium ion during setting. *Food Hydrocolloids, 21*(3), 359–367.

Yu, D., Jiang, Q., Xu, Y., & Xia, W. (2017). The shelf life extension of refrigerated grass carp (Ctenopharyngodon idellus) fillets by chitosan coating combined with glycerol monolaurate. *International Journal of Biological Macromolecules., 101*, 448–454.

Yu, D., Regenstein, J. M., & Xia, W. (2018). Bio-based edible coatings for the preservation of fishery products: A review. *Critical Reviews in Food Science and Nutrition., 59*(15), 2481–2493.

Yuan, J.-L., Lv, Z., Liu, Z.-G., Hu, Z., & Zou, G.-L. (2007). Study on interaction between apigenin and human serum albumin by spectroscopy and molecular modeling. *Journal of Photochemistry and Photobiology A: Chemistry., 191*(2), 104–113.